August 1972 LRP 55/72

CENTRE DE RECHERCHES EN PHYSIQUE DES PLASMAS

FINANCÉ PAR LE FONDS NATIONAL SUISSE DE LA RECHERCHE SCIENTIFIQUE

A DIFFERENTIAL SYSTEM FOR MAGNETIC PROBE MEASUREMENTS

D.W. Ignat

A. Heym

LAUSANNE

August 1972 LRP 55/72

A DIFFERENTIAL SYSTEM FOR MAGNETIC PROBE MEASUREMENTS

D.W. Ignat
A. Heym

Abstract

Use of an integrated circuit differential amplifier and passive RC integration provides magnetic probe signals of large bandwidth untroubled by electric pickup.

Lausanne

potential difference between the two leads of the probe coil, whereas the pickup influences the potentials on the two leads equally. The transformer passes the difference signal, but not the common signal, thereby greatly facilitating the measurement.

The high voltage isolation transformer used had, because of its good electrostatic decoupling, a large leakage inductance of some 20 μHenrys. This inductance combined with any reasonable secondary resistance caused at least partial integration of the signal, so a resistance small enough to allow complete integration of the $\frac{\partial B}{\partial t}$ proportional probe output was used. Because of this small resistance (18 Ω) the transformer did not present a good terminating impedance for the cable coming from the probe coil, and this cable had to be kept short. As a result, any undesired signals entering the long transmission line between the transformer and the oscilloscope were not rejected. The system described above greatly decreased, but did not entirely eliminate, spurious signals. Hope of improving the measurement rested with one or more of the following steps.

1) Improving the transformer system, especially to allow the transformer to be moved inside the cage. Specific goals would be increasing the electrostatic isolation and decreasing the leakage inductance. The frequency response should be extended to lower frequencies.

2) Shielding electrostatically the probe coil itself. This coil is the only point in the measuring chain with no electrostatic shield, and so is a likely source of trouble. Some changes in the probe apparatus would be required, in particular a slight increase in the diameter of the glass envelope.

3) Using a differential amplifier instead of a transformer to process the signal. Such a piece of electronics would naturally

be placed in the cage and could be expected to give better frequency response. The disadvantage would be the addition of another electronic component to the experiment.

The recent availability of cheap integrated circuit differential amplifiers of large bandwidth and high common mode rejection ratio (CMRR) encouraged us to pursue possibility (3) to the exclusion of the others. The scheme envisaged, diagrammed in Fig. 1, is the following. The magnetic probe coil impresses a voltage between two leads of the bifilar transmission line which is composed of a twisted pair of wires running inside a grounded cyclindrical shell or braid. Inside the Faraday cage this transmission line is properly terminated by connecting each lead to ground through a resistor equal to 1/2 the characteristic impedance, thus making the total resistance between the leads fully equal to the characteristic impedance. The signals appearing on the leads are each integrated passively and then combined in a differential amplifier to reject the common mode electric pickup and to retain the differential mode magnetic field signal. The output of the differential amplifier is then fed directly to an oscilloscope input.

Description of the Probe and Transmissions Lines to the Cage

The probe, unchanged from that described previously[2], consists of two nested coils wound of 0.15 mm diameter formvar insulated wire, a solenoidal one meant to measure B_z (pointing along the axis of the probe supporting stem) and, wound inside this one, a "pancake" coil meant to measure B_θ (perpendicular to the stem axis). Both probes have an effective area of approximately 25 mm^2, with the B_z probe having a slightly larger value than the B_θ probe. The nested coils form a cylinder approximately 6 mm long and 2 mm in diameter. The leads of each coil are twisted together and both sets are brought out parallel to the axis of the cylindrical discharge ves-

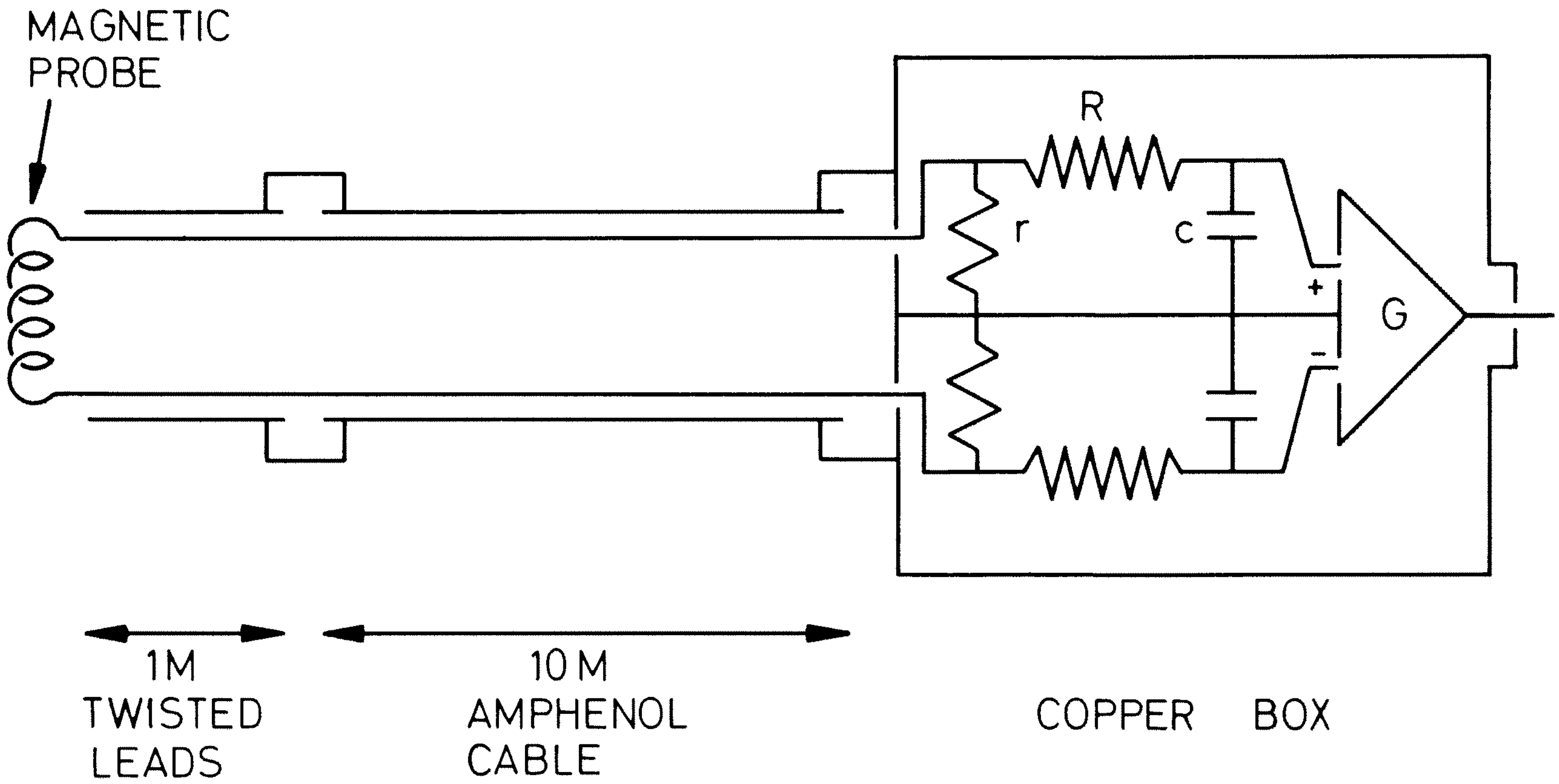

Figure 1: Schematic showing the course of the probe signal from a sensing coil to the differential amplifier output. Each terminating resistance r is equal to one half of the characteristic impedance of the Amphenol bifilar cable. Signal integration is made passively with a time constant of RC and pickup rejection is achieved in the differential amplifier of gain G before feeding the signal to the oscilloscope. In the actual device two nested magnetic coils have their signals carried out of the plasma tube on twisted leads running through the same one meter long hollow copper shield. Thereafter the signals follow separate chanells through the Amphenol cable, integrator and amplifier.

sel through a hollow copper tube of 1.0 mm inside diameter. The entire probe-tube assembly is contained in a glass sheath.

On passing through the end of vacuum chamber each pair of probe leads is soldered to a BNC-type bifilar connector[3] and the copper tube shield is attached to the connector body. From this point RG-108A/U[4] cable, running for the most part inside additional double shielding, carries the signal to a proper termination inside the Faraday cage.

The twisted probe leads, together with the hollow copper tube, form a transmission line of rather high ($\sim 100\ \Omega$) characteristic impedance. This was determined by J.-M. Peiry from separate measurements of the open circuit capacitance and closed circuit inductance per unit length[5]. The twisted lead transmission line joins the Amphenol cable, which is presumed well terminated. We wish an estimate of the effect of the resulting mismatch.

To this end we idealize the system as follows: the probe is a voltage source supplying $V_B e^{i\omega t}$, in series with its self-inductance L. The probe feeds a transmission line of length ℓ, impedance Z, and phase velocity v_p which is terminated in Z_o. Application of the transmission line equations yields for the voltage applied to the load Z_o:

$$V_{LOAD} = V_B \left\{ e^{\frac{i\omega\ell}{v_p}}\left(1 + \frac{i\omega L}{Z_o}\right) + i\sin\left(\frac{\omega\ell}{v_p}\right)\left(\frac{Z - Z_o}{Z Z_o}\right)\left(Z - i\omega L\right) \right\}^{-1} \qquad (1)$$

Since $L \cong .1\mu$ Henry, and $\omega L \cong 3$ ohms at 5 MHz, we neglect ωL. Further with $\frac{\omega}{2\pi} = 5$ MHz, $\ell = 1$ m, $v_p = 2 * 10^8$ m/s, the sine may be replaced by its argument. For faithful transmission, then, we require

$$\left| \frac{\omega\ell}{v_p}\left(\frac{Z - Z_o}{Z_o}\right) \right| \lesssim .1 \qquad (2)$$

For the values assumed and quoted above, Eqn. (2) becomes $0.04 < .1$ and is therefore satisfied. We wish to make the point, however, that it is not overwhelmingly satisfied, and that were $\ell = 2$ m and $Z = 160\ \Omega$, one would have a troublesome impedance problem.

We conclude that the lack of care in the electrical design of the connection between the probe and Amphenol transmission line is probably permissible. Experimental evidence on this point will be given later.

Description of the Box Containing Cable Termination, Integrator and Electronics

Ten meters of Amphenol bifilar cable carry the signals into the Faraday cage. There the cable connects to a copper box attached directly to the oscilloscope preamplifier, in which the cable is terminated, signal integrated, and then processed with differential amplifier circuitry (see Fig. 2). The power supplies required are external. The cable is terminated by connecting each lead to ground through a high voltage hollow composition resistor[6]. Each resistor is trimmed with normal composition resistors running outside it so the parallel combination of trimmer, composition resistor, integrating resistor, is equal to 39 ohms. Then 78 ohms, the cable characteristic impedance, is placed across the bifilar leads. The integrating resistor is a series connection of 5 composition resistors each of about 1.8 KΩ impedance and runs through the middle of the terminating resistor. Due to such construction nearly all stray capacity associated with the integrating resistor runs to the terminating resistor. Since the impedance of the integrating capacitor is small, there is practically no voltage difference between the integrating and terminating resistors all along their lengths. Therefore the stray capacity is not charged and plays no role[7]. The two integrating resistors are carefully

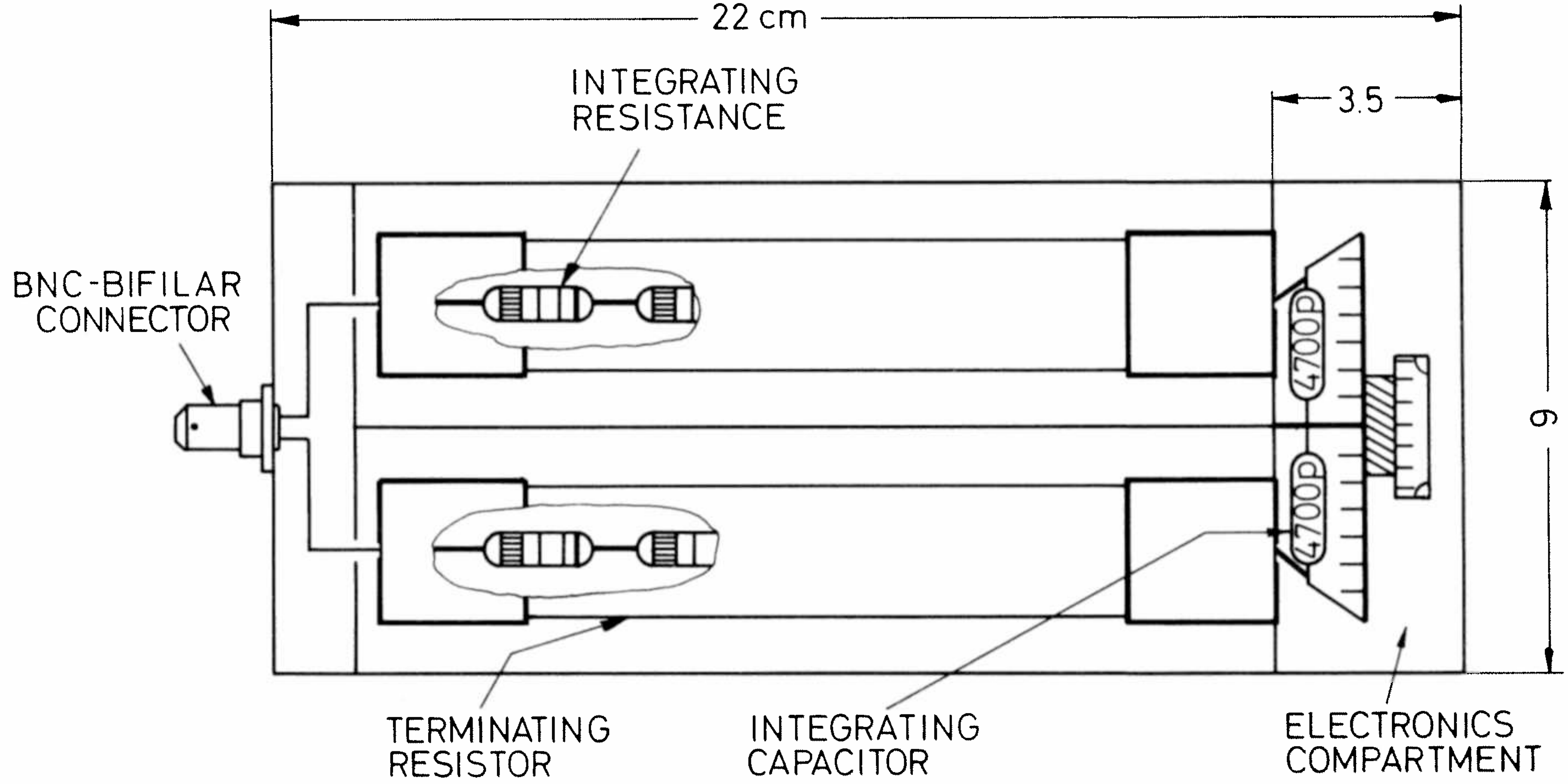

Figure 2: Sketch of the uncovered copper box showing the two hollow terminating resistors with the integrating resistor running inside, the integrating capacitors which are each a parallel combination of two 4700 pf polyester capacitor, and the electronics as vector board mounted.

matched with a bridge and have a value of about 9 kΩ.

This value of R was chosen as one which would not be expected to give trouble with stray capacity. It is also one which does not put overly strenuous requirements on the input impedance of the electronics to follow.

The terminating and integrating resistors are in one electrical compartment of the copper box. The integrating capacitor and the electronics are in another with the connection made through a small hole. Each integrating capacitor is an inductance minimizing parallel combination of 2 polyester 4700 pf condensers rated for 400 volts, thus making nominal time constants of 85 μ seconds.

The central electronic component is an integrated circuit, broad band differential amplifier (Texas Instruments SN7510N) with complementary outputs whose important characteristics include: frequency response, DC to 40 MHz; voltage gain, x 100; common mode rejection ratio, 85 db; and input impedance 6 KΩ.

A high input impedance field effect transistor stage was required between the integrator and the differential amplifier to avoid loading the integrator. The complementary outputs allowed resistive feedback across the amplifying stage in order to stabilize the overall gain against variation of the exact values of the transistor parameters. Great care was taken in decoupling the power supply by placing .1 μ farad capacitors to ground at the point of voltage feed to the solid state components, and inserting 47 Ω between this point and the entrance of supply power into the copper box. A schematic of the circuit is shown in Fig. 3.

The resistive feedback did tend to cause the circuit to oscillate at frequencies between 10 and 40 MHz. The oscillation could be eliminated with careful placement of pico-farad sized capacitors,

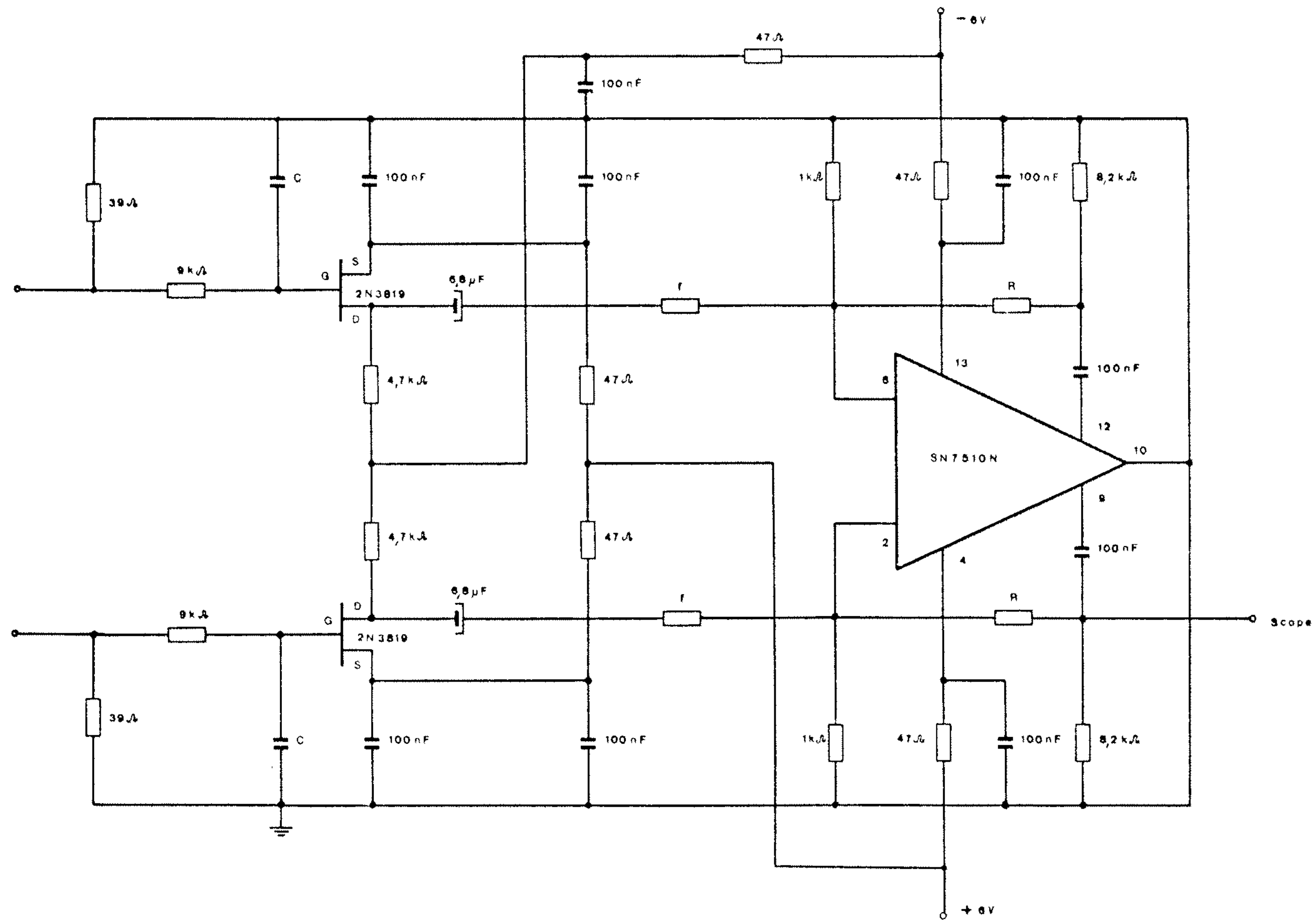

Figure 3: Circuit diagram of the fedback differential amplifier with the preceding high impedance field effect transistor stage, integrating resistance (9 Kohm) and cable terminating resistance (39 ohm). The resistances labled R and r are respectively the feedback and input resistors on the differential amplifier.

formed by twisting insulated wires together, across the feedback resistor labeled R. However, with the physical layout used now (Fig. 4) the oscillation without any deliberate shunt capacity across R is so small that it was allowed to remain. Evidence of the remaining oscillation can be seen especially on the rapidly changing portions of the magnetic probe oscilloscope traces.

The integrated and differentially processed signal exits through a BNC male connector which allows the box to be fitted directly to the oscilloscope input.

Performance of The Integrator Box

In checking the performance of the integrator and associated electronics we feed a balanced signal from a signal generator followed by an r.f. isolation transformer to the input BNC-type bifilar connector. A Tektronix high impedance probe senses the signal at one or the other of the inputs for display on one channel of a double beam oscilloscope while the box output drives the second beam. Polaroid photographs of the double display allow careful determination of the voltage gain and phase shift. A log-log plot of the voltage gain versus frequency for one of the two integrators appears in Fig. 5. Experimental data are plotted as points and an ideal integrator curve of appropriate gain is shown as a straight line. The frequency $f_{c.o.}$ at which the amplitude response has dropped to $\frac{1}{\sqrt{2}}$ of the ideal response defines the time constant RC through

$$RC = \frac{1}{2\pi f_{c.o.}}$$

Accordingly, the inferred time constant is about 80 μ seconds, and the overall electronic gain is about 2.5. The high frequency

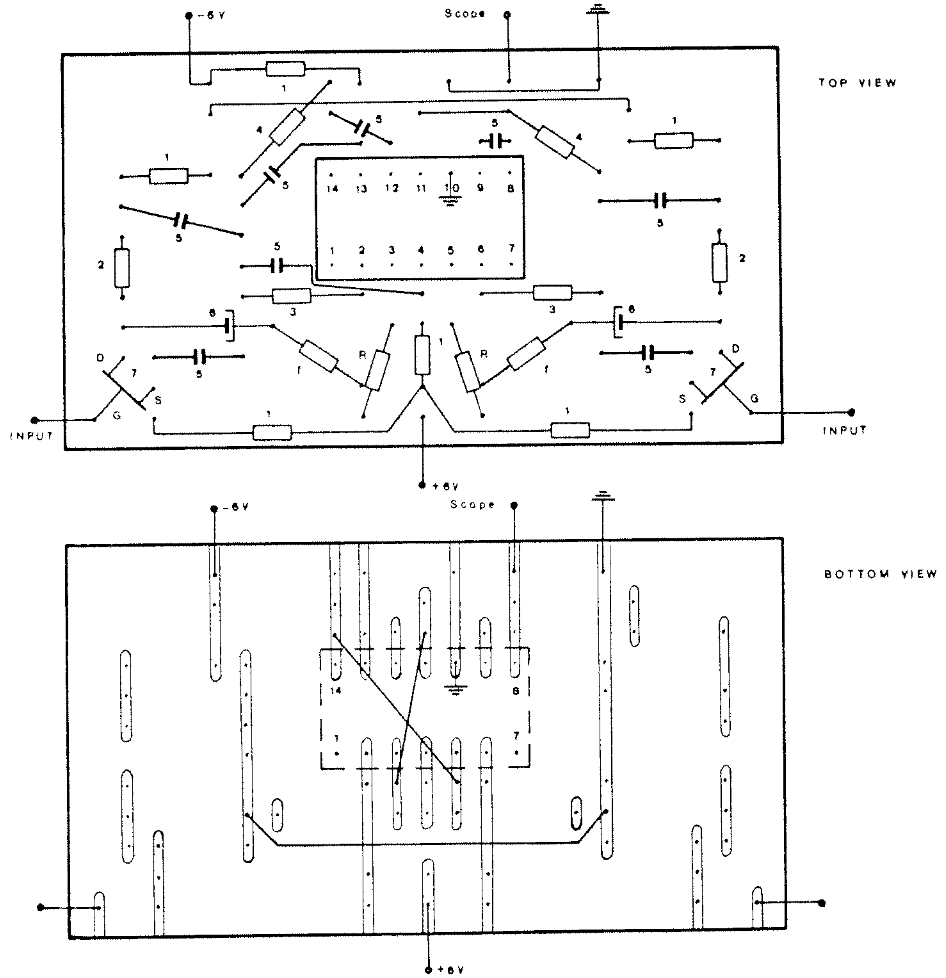

RESISTORS

REF N°	DESCRIPTION	
N°1	47Ω	1/8W
N°2	4,7 kΩ	"
N°3	1 kΩ	"
N°4	8,2 kΩ	"
N°R	4,7 kΩ	"
N°f	470Ω	"

CAPACITORS

REF N°	DESCRIPTION
N°5	100nF
N°6	6,8μF

TRANSISTORS

REF N°	DESCRIPTION
N°7	FET 2N3819

INTEGRATED CIRCUIT

REF N°	DESCRIPTION
	SN7510N

Pins 1,7,8,14 have no internal connection to the integrated circuit

Figure 4: The exact physical layout for the electronic components on a vector board measuring 5.8 cm by 3.0 cm. The integrators are not shown here. This particular layout allowed only very low level high frequency oscillation due to the feedback, and was usable as shown.

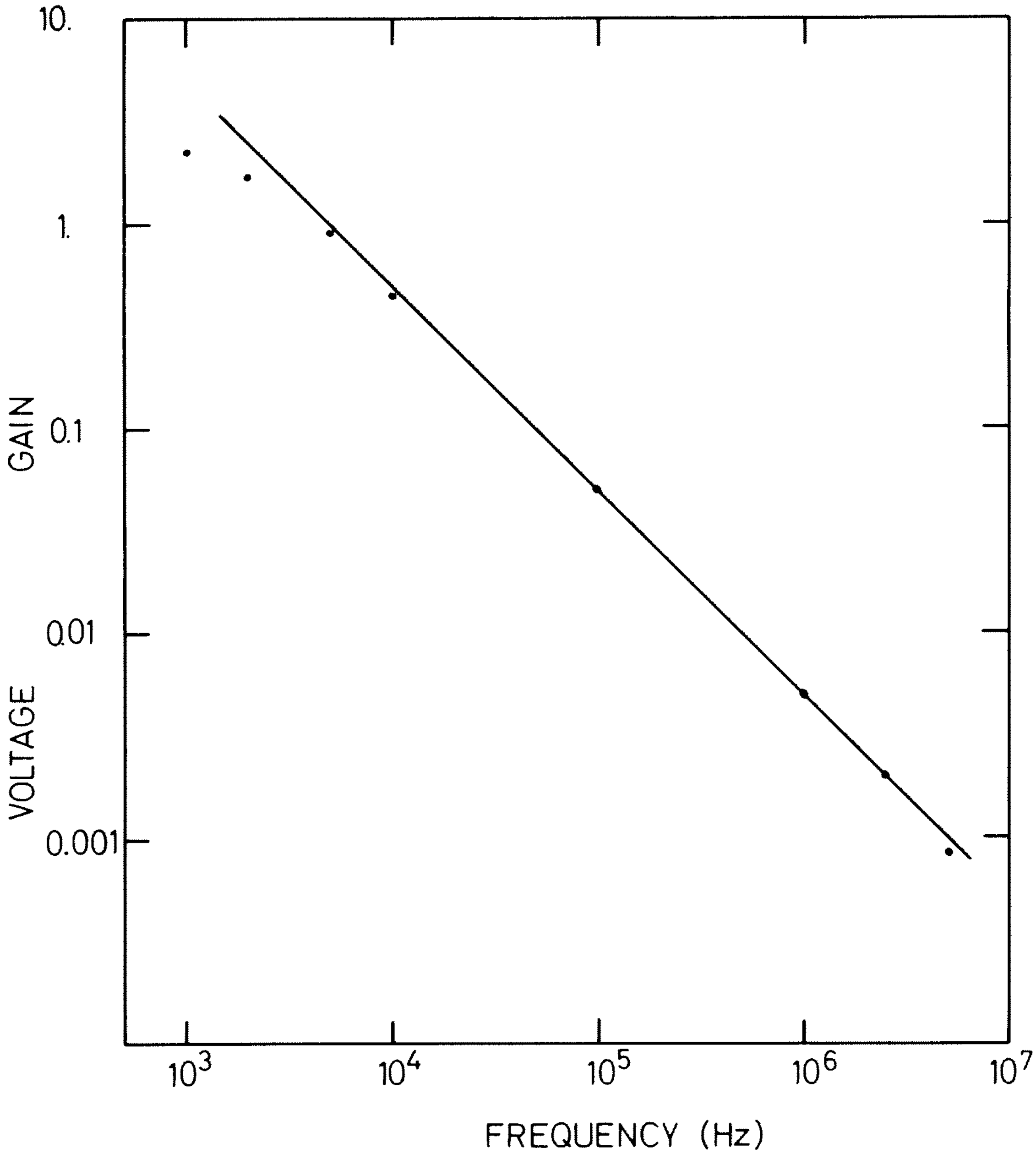

Figure 5: Overall voltage gain of the integrator and differential amplifier combination as a function of frequency showing experimental points and the best fitting ideal integrator characteristic. The low frequency cutoff at about 2 kHz means a time constant of about 80 μ sec. The high frequency cutoff above 5 MHz is caused by the integrating capacitor resonating with is its residual self-inductance.

response has deteriorated noticeably at 5 MHz. The unavoidable self inductance in the integrating capacitor and its connections resonate with the capacity around 12 MHz and thus influences the circuit behaviour at 5 MHz.

By lowering the integrating capacity, so that the L-C resonance frequency would rise, the frequency response above 5 MHz could be improved, but at the expense of the low frequency response. Due to the unexpectedly large low frequency magnetic fields measured in the experiment, we decided that the selection of components as above was a healthy compromise.

After time constant, gain, and high frequency cut off, the most important electrical parameter is the common mode rejection ratio (CMRR). In Fig. 6 this quantity is graphed versus frequency in a log-log manner. The signal reaching the oscilloscope at high frequencies when both input leads are driven in phase is nearly the same whether or not the electronics is energized. This means that the common mode rejection is limited by direct coupling through the integrator box.

Performance of the overall system

The sensitivity calibration for the magnetic measurement was made with the entire system assembled. The magnetic probe is inserted into the field of a Helmholtz pair (10 cm diameter) energized by a Rhode-Schwartz oscillator with the aid of parallel ringing capacitors whose size depends on the frequency of interest. The probe signal then proceeds one meter on the twisted filaments inside the copper tube, 10 meters on the RG108A/U, entering the integrator box in the cage, and finally to a high input impedance Rhode Schwartz μ-voltmeter. The signal here is compared with that from a standard probe (formed of a single turn of fine wire wound

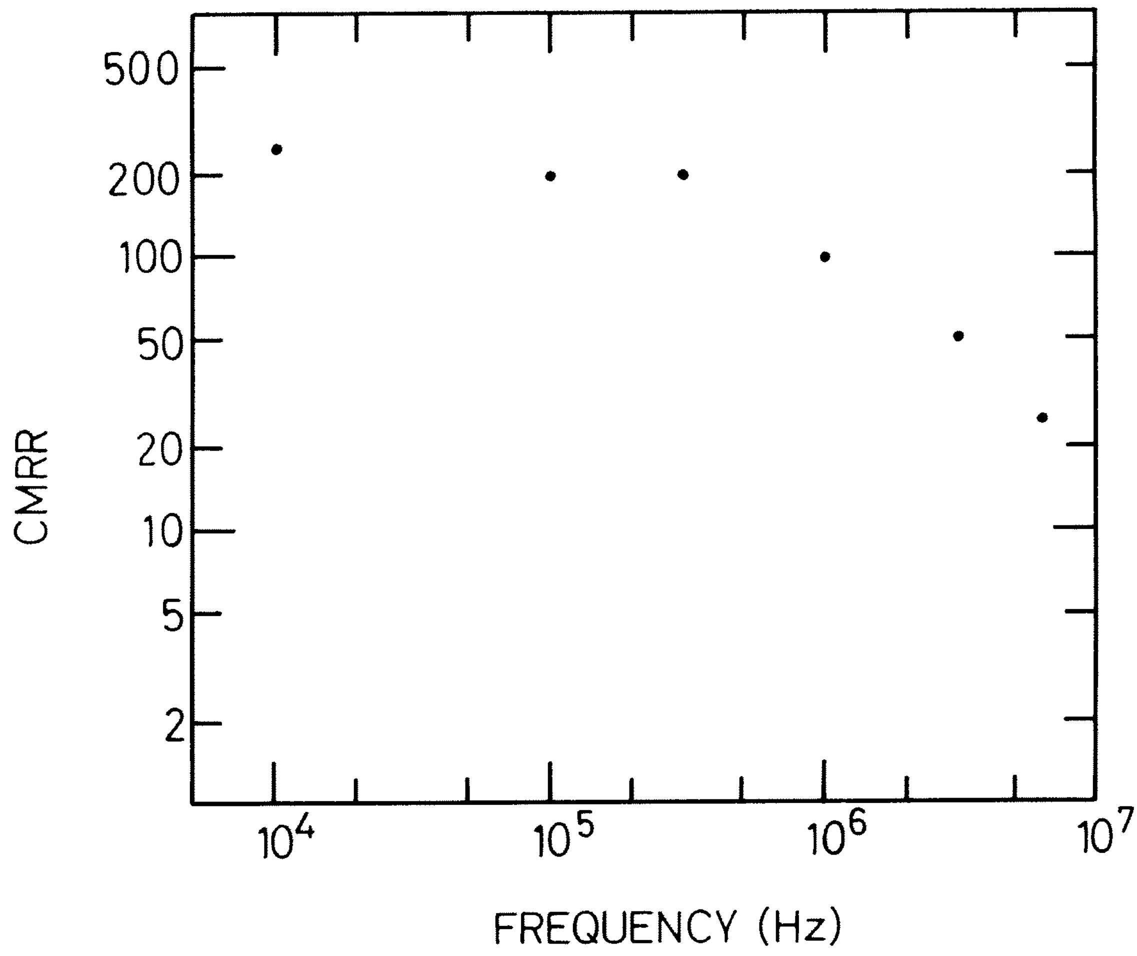

Figure 6: Common mode rejection ratio (CMRR) versus frequency for the apparatus. At high frequency this quantity is governed by the direct coupling through the copper box.

on a 1 cm diameter glass form and connected immediately to a 50 ohm coaxial cable) measured on the same voltmeter but with 50 ohms input impedance. The area of the standard has been calibrated as a function of frequency by J.-M. Peiry with the aid of an accurately machined standard inductor to measure the current flowing in the Helmholz coil[8]. One can thus obtain the sensitivity of the experimental probe combined with cables and electronics for any frequency, and if the transfer function of the integrator box is known, the effective area of the coil can be expressed. Fig. 7 shows the variation of the effective area of a B_θ coil assuming the integrator- amplifier transfer characteristic measured at 2.5 MHz behaves ideally for other frequencies. The error bars partly reflect variations in measurement results when reading the needles of the voltmeter and partly uncertanties in various quantities. This measured effective area includes losses and mismatches in the transmission lines as well as possible variations in probe area.

In Fig. 8 one sees how the system works in the experiment. We placed the double probe at 50 mm from the wall of the discharge tube, or 25 mm from the center, then made discharges of the r.f. line in 20 mTorr of deuterium. Each photograph carries on top the trace from interior magnetic probe and on the bottom the trace from the external total current probes which indicate the magnetic field existing at the wall of the discharge. The two most left photos show B_θ; the most right show B_z. The top two photos represent the situation when the differential amplifier circuitry is functioning properly; the bottom two show the result of artificially eliminating the common mode rejection capability. The external current probe is left unchanged.

One can see that this method of detection greatly facilitates the measurement.

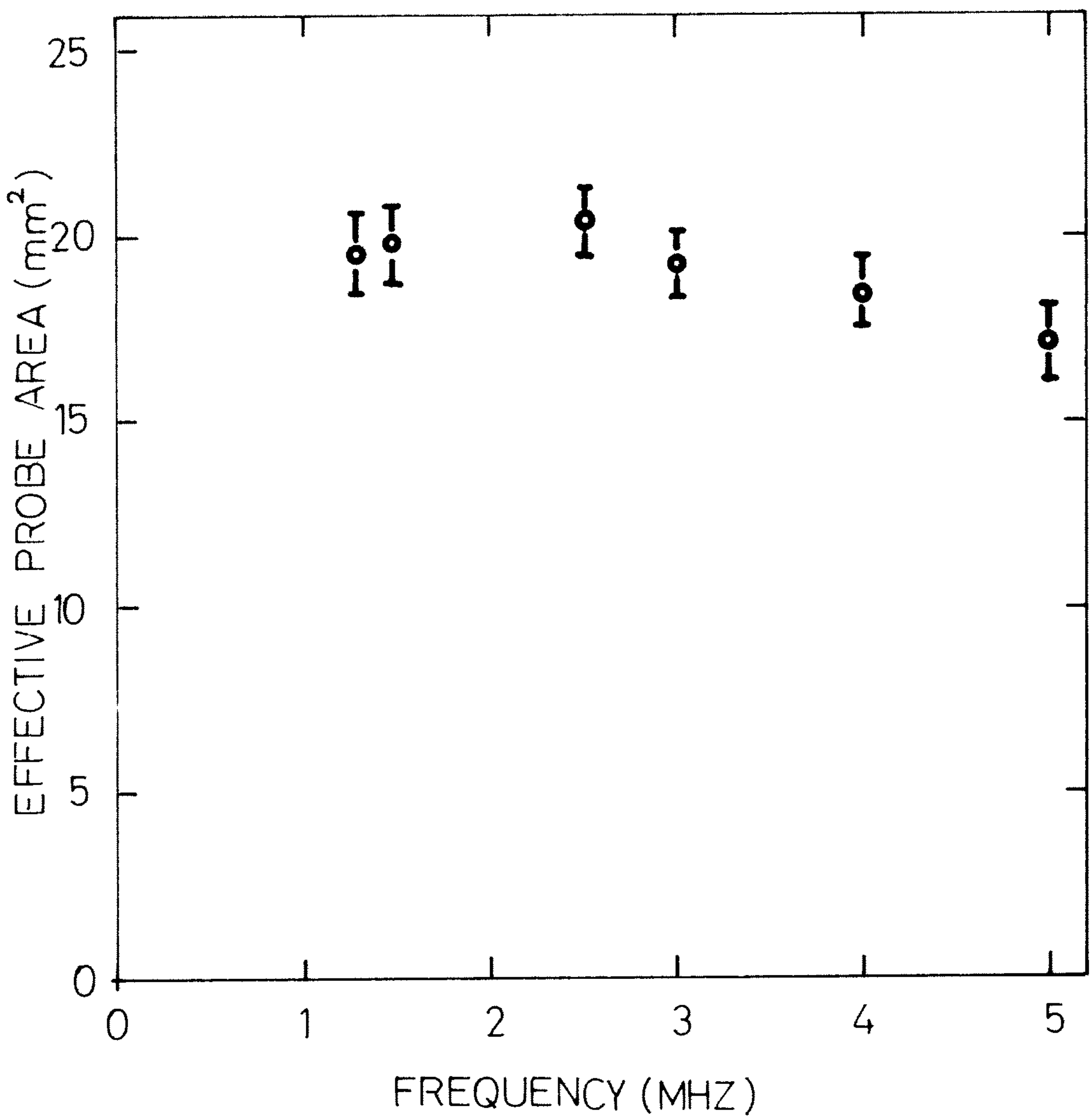

Figure 7: An example of the frequency dependence of the effective area of the magnetic probe with the entire measuring chain considered as a whole. The effect of cable mismatching is included as well as variations in the effective area of the probe coil.

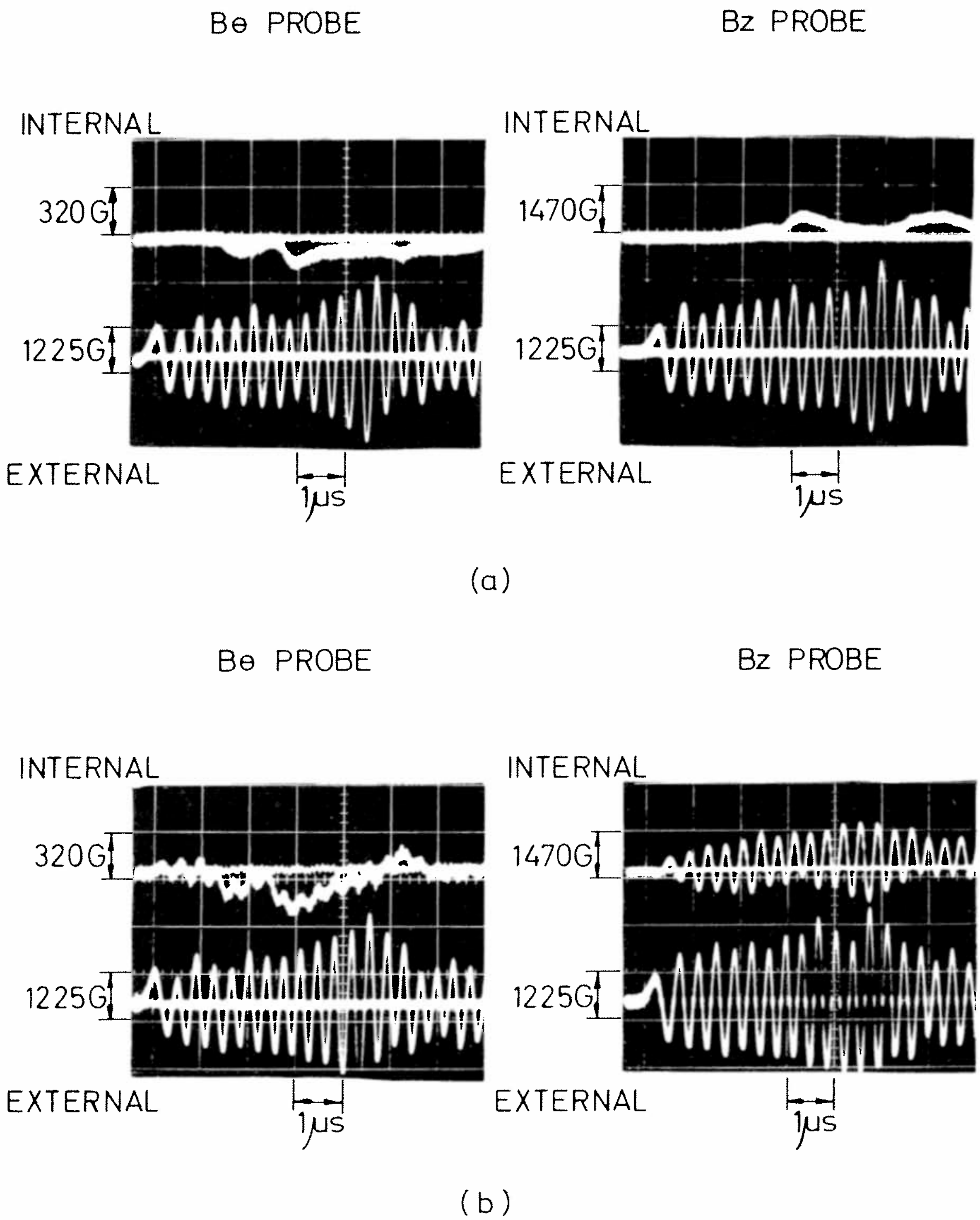

Figure 8: A series of oscilloscope traces illustrating the improvement on the internal magnetic field measurement allowed by the differential amplifier system (a) over a similar system with no common mode rejection capability (b).

Remarks on the choice of time constants

Consider the simple RC integrator.

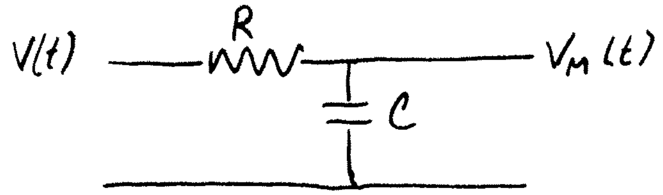

Elementary circuit equations yield

$$V_M(t) = \frac{1}{RC}\int_0^t V(t')\exp\left(-\frac{(t-t')}{RC}\right)dt' \tag{3}$$

and one sees that the integration error is

$$V_M(t) - \frac{1}{RC}\int_0^t V(t')dt' = \frac{1}{RC}\int_0^t V(t')\left[\exp\left\{-\frac{(t-t')}{RC}\right\} - 1\right]dt' \tag{4}$$

The integration error is certainly small if (1) RC is much greater than the time of observation, or (2), if V(t) changes symmetrically about zero often in a time RC. Of course a combination of the two conditions is possible. In previous measurements of the magnetic field inside the plasma, one relied on condition (2) to keep the integration error small. RC was chosen to be about 1.3 μ sec which was considerably smaller than the duration of the experiment (~7 μ sec. to discharge the r.f. line), but was larger than the r.f. period (.4 μ sec.). Recent measurements have disclosed the existence of magnetic fields which change little in a microsecond, and thus time constants much larger than the 7 μ sec. line discharge time are required.

Once these longer time constants are introduced a new problem emerges. The preionization, lasting a total of 15 μ sec., is a twice repeated z-pinch which naturally produces a B_θ field having low frequency components. These B_θ fields are sensed by the interior magnetic probe. Therefore, as far as the B_θ probe is concerned, the observation time is over 20 μ sec., and in principle a time constant much larger than this is required. As discussed in the text, we were not able to easily attain integration times over 80 μ sec. without damaging the high frequency response of the probe system.

Fortunately, in the actual experiments the integration error, while being observable, was not found to be important when using 80 μ sec. time constants.

Remarks on Possible Improvements and Changes

The system as described works adequately for the experiment at hand. The three important electrical parameters (1) low frequency cut off at 3 kHz (2) high frequency cut off slightly above 5 MHz (3) common mode rejection ratio about 50 at 2.5 MHz are each very close to the limit of acceptability, and future modifications in the characteristics of the rotating magnetic field pinch may force improvement of one or more electrical parameters of the differential integrating system.

A ten fold increase in the integrating resistor will, if the problem of stray capacity does not become important, allow smaller integrating capacitors, with a reduced problem of LC resonance.

The best theoretical solution to the frequency response problem is the use of a true electronic differential integrator, either a Miller integrator or a bootstrap. Both such solutions were tried, but self oscillation of the circuit at high frequencies was an unsolvable problem (for us).

Improved CMRR can probably be achieved only with an electrically tighter construction of the copper box.

Elimination of the feedback on the differential amplifier will increase the overall voltage gain 20 fold, at the cost of gain stability against component aging, temperature drifts and transistor replacement.

Conclusion

We have conceived, constructed, and tested a new system depending on integrated circuit differential amplifiers for obtaining magnetic probe measurements uncontaminated by electric pickup. This system is particularly useful in the environment of the rotating magnetic field pinch where the high frequencies and power levels have made conventional magnetic probe measurements difficult. Low frequency response to 3 kHz has been possible, as well as necessary. The shortcomings of the system and possibilities for future improvement have been mentioned.

Acknowledgements

This work was supported by the "Fonds National Suisse de la Recherche Scientifique".

Figure Captions

Figure 1: Schematic showing the course of the probe signal from a sensing coil to the differential amplifier output. Each termimating resistance r is equal to one half of the characteristic impedance of the Amphenol bifilar cable. Signal integration is made passively with a time constant of RC and pickup rejection is achieved in the differential amplifier of gain G before feeding the signal to the oscilloscope. In the actual device two nested magnetic coils have their signals carried out of the plasma tube on twisted leads running through the same one meter long hollow copper shield. Thereafter the signals follow separate channels through the Amphenol cable, integrator and amplifier.

Figure 2: Sketch of the uncovered copper box showing the two hollow terminating resistors with the integrating resistor running inside, the integrating capacitors which are each a parallel combination of two 4700 pf polyester capacitors, and the electronics as vector board mounted.

Figure 3: Circuit diagram of the fedback differential amplifier with the preceding high impedance field effect transistor stage, integrating resistance (9 Kohm) and cable terminating resistance (39 ohm). The resistances labled R and r are respectively the feedback and input resistors on the differential amplifier.

Figure 4: The exact physical layout for the electronic components on a vector board measuring 5.8 cm by 3.0 cm. The integrators are not shown here. This particular layout allowed only very low level high frequency oscillation due to the feedback, and was usable as shown.

Figure 5: Overall voltage gain of the integrator and differential amplifier combination as a function of frequency showing experimental points and the best fitting ideal integrator characteristic. The low frequency cutoff at about 2 kHz means a time constant of about 80 μ sec. The high frequency cutoff above 5 MHz is caused by the integrating capacitor resonating with is its residual self-inductance.

Figure 6: Common mode rejection ratio (CMRR) versus frequency for the apparatus. At high frequency this quantity is goverened by the direct coupling through the copper box.

Figure 7: An example of the frequency dependence of the effective area of the magnetic probe with the entire measuring chain considered as a whole. The effect of cable mismatching is included as well as variations in the effective area of the probe coil.

Figure 8: A series of oscilloscope traces illustrating the improvement on the internal magnetic field measurement allowed by the differential amplifier system (a) over a similar system with no common mode rejection capability (b).

Footnotes

(1) The most recent publication on this experiment is: A. Berney, A. Heym, F. Hofmann and I.R. Jones, Plasma Physics 13, 611 (1971). Further references are contained therein.

(2) I.R. Jones, J.-M. Peiry and D. Cocq, Rev. Sci. Instrum. 40, 133 (1969).

(3) The Amphenol part numbers for these pieces are: panel connector, 31-235; cable connector, 31-222.

(4) The cable used is Amphenol part number 21-327. Important parameters quoted by Amphenol are: characteristic impedance, 78 Ω; Capacity per meter, 77.1 μ F; phase velocity 0.68 C. The cable-connector combination is designed for applications below 100 MHz.

(5) I.R. Jones, J.-M. Peiry and D.Cocq, Report No LRP 35/67 (December 1967), this Laboratory.

(6) Specifically, Morganite Heavy Duty Carbon Resistors, Tube Type, part number 4702 having a nominal value of 50 Ω (Morganite Resistors Limited, England). These resistors are 15 cm long, having 1.5 and 2.5 cm inside and outside diameter respectively. They are chosen for their low inductance and high voltage rating for pulsed operation (800 v/cm).

(7) R. Keller, Rev. Sci. Instrum. 35, 1057 (1964), see page 1058.

(8) E.S. Weibel, Report No LRP 50/71 (November 1971) this Laboratory.